

CHARGE INHOMOGENEITIES IN THE COLOSSAL MAGNETORESISTANT MANGANITES FROM THE LOCAL ATOMIC STRUCTURE

S. J. L. BILLINGE*, V. PETKOV*, TH. PROFFEN*, G. H. KWEI**, J. L. SARRAO**, S. D. SHASTRI*** and S. KYCIA****

*Center for Fundamental Materials Research and Department of Physics and Astronomy, Michigan State University, East Lansing, MI 48824.

**Los Alamos National Laboratory, Los Alamos, NM 87545

***Advanced Photon Source, Argonne National Laboratory, Argonne, IL

****Cornell High Energy Synchrotron Source, Ithaca, NY

ABSTRACT

We have measured atomic pair distribution functions (PDF) of $\text{La}_{1-x}\text{Ca}_x\text{MnO}_3$ using high energy x-ray diffraction. This approach yields accurate PDFs with very high real-space resolution. It also avoids potential pitfalls from the more usual neutron measurements that magnetic scattering is present in the measurement, that the neutron scattering length of manganese is negative leading to partial cancellation of PDF peaks, and that inelasticity effects might distort the resulting PDF. We have used this to address the following questions which do not have a satisfactory answer: (1) What are the amplitudes and natures of the local Jahn-Teller and polaronic distortions in the CMR region. (2) Is the ground-state of the ferromagnetic metallic phase delocalized or polaronic. (3) As one moves away from the ground-state, by raising temperature or decreasing doping, towards the metal insulator transition, how does the state of the material evolve?

INTRODUCTION

A very large magnetoresistance is observed in the, so-called, colossal magnetoresistant manganites [1]. This coupling of magnetic field to transport is qualitatively understood using the concept of double exchange [2]. That this description underlies the CMR phenomenon appears not to be in question [3]. However, the DE model has difficulty to account quantitatively for the observed T_c 's and the magnitude of the resistivity change at T_c , and is totally incapable of explaining the complex phenomenology away from the ideal CMR compositions [4,5]. A number of authors [4,6–10] have suggested that the extra contribution to the model should be an electron-lattice coupling term. Extensive experimental evidence exists for lattice effects in these materials. For example, anomalous increases in crystallographic Debye-Waller factors [11] and, equivalently, PDF peak-widths [12] and XAFS Debye-Waller factors [13,14] at the MI transition; an oxygen isotope dependence to T_c [15,16]; thermal conductivity [17,18] and transport measurements above T_c interpreted in terms of polaron dynamics [19,20]. These results can be consistently interpreted if charges localize as small polarons above T_c .

Early work using a number of different techniques [11–13,15,21] established the importance of the lattice to the colossal magnetoresistance phenomenon. More recently attention has been focussed on understanding the precise *nature* of the polaronic state and the related Jahn-Teller distortions. We have concerned ourselves with a number of questions: (1) What does the polaronic distortion look like? (2) What is the ground-state of the ferromagnetic metallic (FM) phase? (3) How do the polarons and Jahn-Teller (JT) distortions evolve with compositional and temperature changes?

The principle result which we have obtained as a result of these studies is that the ferromagnetic metallic phase of $\text{La}_{1-x}\text{Ca}_x\text{MnO}_3$ is *microscopically* inhomogeneous [22,23]. This is in accord with a number of other experimental and theoretical observations [7]. It is particularly interesting in light of the observation of *macroscopic* phase coexistence in materials with a smaller A-site ion size, $\langle r_A \rangle$ [24,25]. The temperature dependence of the local structure in $\text{La}_{1-x}\text{Ca}_x\text{MnO}_3$ is characteristic of regular phase separation phenomena with two phases coexisting and the proportion of each phase evolving with changing temperature or doping. However, in this system *no macroscopic phase coexistence is observed*: it is a purely local structural phenomenon. The relative proportion of the sample in the localized and delocalized states can be quantified using the PDF as we describe below. The results are compared to earlier neutron PDF results.

EXPERIMENTAL

Samples of $\text{La}_{1-x}\text{Ca}_x\text{MnO}_3$ with $x = 0.0, 0.12, 0.21, 0.25$ and 0.33 , were synthesized by standard solid-state reaction. Details are reported elsewhere [22]. X-ray powder diffraction data were collected out at the A2 24 pole wiggler beam line at Cornell High Energy Synchrotron Source (CHESS) and at beamline BM1 at the Advanced Photon Source (APS). The measurements were made in flat-plate symmetric-transmission geometry. Finely ground powders of uniform thickness ~ 5 mm were supported between thin kapton foils on the cold-finger of a helium displax refrigerator. The sample thickness was determined so that the absorption of the sample was $\mu t \sim 1$. Xrays of energy 60 keV and 65 keV were used at CHESS and APS, respectively. The raw data were corrected for experimental effects such as absorption and multiple scattering. Unwanted scattering such as backgrounds and Compton scattering were removed, and the data were normalized to obtain the total scattering factor, $S(Q)$, where Q is the magnitude of the momentum transfer ($Q = 4\pi \sim \theta/\lambda$). $S(Q)$ is defined as

$$S(Q) = 1 + \frac{I_{el}(Q) - \sum_i c_i f_i^2(Q)}{[\sum_i c_i f_i]^2} \quad (1)$$

where I_{el} is the measured elastic part of the spectrum, c_i and $f_i(Q)$ are the atomic concentration and scattering factor of the atomic species of type i ($i = \text{La, Ca, Mn and O}$), respectively [26]. The data processing was carried out using the program RAD [27]. The PDF is obtained from $S(Q)$ by a direct Fourier transform according to

$$G(r) = \frac{2}{\pi} \int_0^\infty Q[S(Q) - 1] \sin(Qr) dQ, \quad (2)$$

The $F(Q) = Q[S(Q) - 1]$ and $G(r)$ functions from the $x = 0.33$ sample collected at 20 K are shown in Fig. 1. The low- r regions of the PDF from this, and various other, data sets are superimposed on the phase diagram in Fig. 2

Data are modeled by calculating the PDF from a model structure. Model parameters are then varied in such a way as to optimize the agreement between the calculated and data-PDFs [29]. The program PDFFIT was used [30]. The solid line in Fig. 1(b) shows the PDF obtained from the average crystal structure refined to the $x = 0.33, 20$ K data-set.

RESULTS

Nature of the Jahn – Teller distortion :

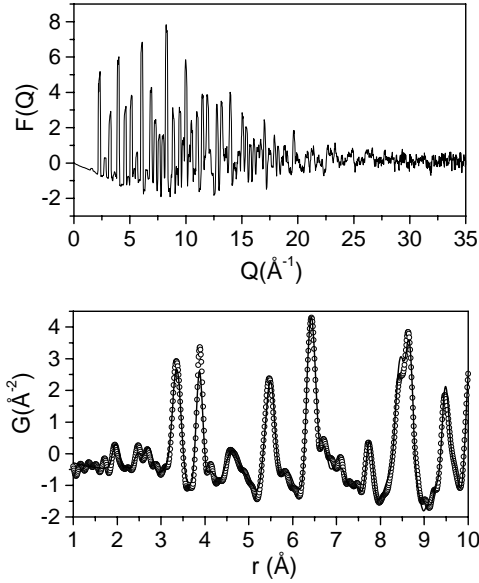


FIG. 1. (a) Total structure function, $S(Q)$, and (b) Reduced radial distribution functions, $G(r)$, for $\text{La}_{1-x}\text{Ca}_x\text{MnO}_3$, $x = 0.33$ at 20 K. In (b) the data are shown as open circles. The solid line is a fit of the average structure to the data. [28]

Undoped LaMnO_3 is insulating. The Mn^{3+} ions are orbitally ordered and the full Jahn-Teller distortion can be measured crystallographically [31–33]. We have verified that the local Jahn-Teller distortion is *quantitatively* the same as the average one [28]. This establishes nature of the local Jahn-Teller distortion around Mn^{3+} in the absence of strain. It also establishes the accuracy of our fitting programs. We have repeated this fit on the present room temperature x-ray data for $x = 0$. The results are summarized in Fig. 3 and Table I. The reproducibility of the results from the x-ray and neutron measurements is excellent as can be seen in Tab. I. The Jahn-Teller distorted octahedra have four short bonds, two each of length 1.92 Å and 1.97 Å, respectively, and two long-bonds of length 2.15 Å.

Evolution of polarons with T and x :

The presence of JT distorted octahedra implies the presence of Mn^{3+} ions whereas doped charges which delocalize result in all the MnO_6 octahedra being undistorted [34]. Thus, using the PDF we can search for evidence of locally Jahn-Teller distorted octahedra which indicate that, in that region of the sample, doped charges are absent or are localized as distinct Mn^{4+} species.

Within the sensitivity of our measurement there is no detectable structural disorder and no local Jahn-Teller distortions are present deep in the FM phase [22,23]. However, as the MI transition is approached, small polarons do appear. We can identify two kinds of phase: a charge localized (Jahn-Teller) phase and a delocalized (Zener) phase which is structurally ordered. We have made a qualitative survey of the phase diagram of $\text{La}_{1-x}\text{Ca}_x\text{MnO}_3$ to search for the presence of JT long-bonds indicating localized material. In Fig. 2 we have superimposed on the electronic phase diagram the region of the PDFs showing the Mn-O short and long bonds [22]. Deep in the FM

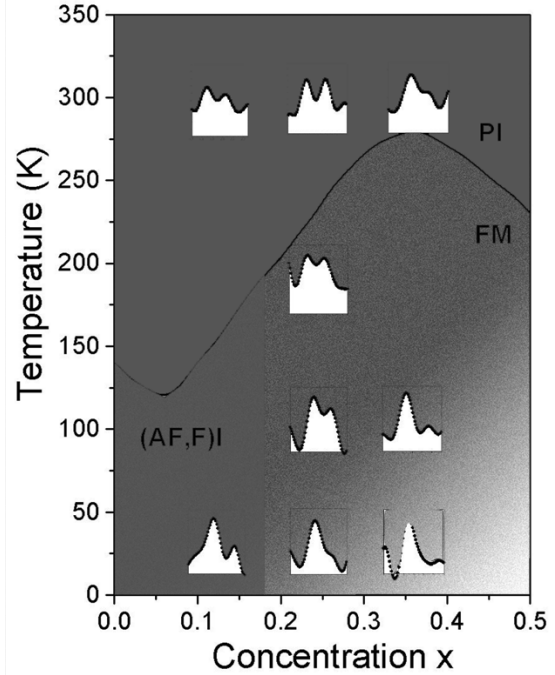


FIG. 2. Phase diagram for $\text{La}_{1-x}\text{Ca}_x\text{MnO}_3$ with high-resolution x-ray PDFs superimposed. The region of the PDF showing the Mn-O nearest neighbor bonds is shown. The speckled pattern indicates the sample is microscopically inhomogeneous in this region [22].

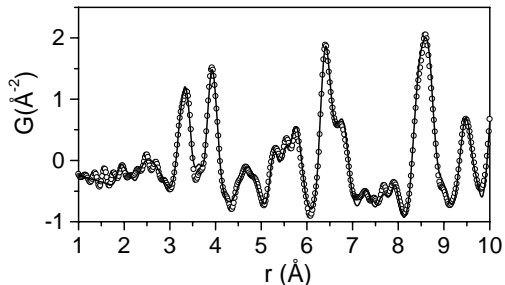


FIG. 3. PDF from LaMnO_3 at 300 K from x-ray data taken at APS. Solid line is a fit of the crystallographic model

	Rietveld	IPNS (neutron)	APS (X-ray)
a	5.542(1)	5.5422(7)	5.5241(9)
b	5.732(1)	5.7437(8)	5.6769(11)
c	7.6832(2)	7.690(1)	7.6865(11)
x(La)	-0.0068(3)	-0.0073(2)	-0.0069(3)
y(La)	0.0501(3)	0.0488(2)	0.04345(17)
$\langle u^2 \rangle$ (La)	0.0022(4)	0.00199(4)	0.00564(5)
$\langle u^2 \rangle$ (Mn)	0.0011(6)	0.00067(7)	0.00713(10)
x(O1)	0.0746(4)	0.0729(3)	0.077(3)
y(O1)	0.4873(4)	0.4857(3)	0.494(3)
$\langle u^2 \rangle$ (O1)	0.0031(5)	0.00233(7)	0.0333(18)
x(O2)	0.7243(3)	0.7247(3)	0.7249(22)
y(O2)	0.3040(3)	0.3068(3)	0.2952(17)
z(O2)	0.0390(2)	0.0388(3)	0.0463(17)
$\langle u^2 \rangle$ (O2)	0.0030(4)	0.00378(5)	0.0201(6)
R_{wp}	12.1	16.2	10.9

TABLE I. Structural data of LaMnO_3 ($Pbnm$) from Rietveld and PDFFIT refinements of neutron powder diffraction data at 20 K [28] and a PDF-FIT refinement of the room temperature x-ray data from APS. La and O1 are on $(x, y, \frac{1}{4})$, Mn is on $(0, \frac{1}{2}, 0)$ and O2 is on (x, y, z) . The units for lattice parameter are Å and for $\langle u^2 \rangle$, Å^2 .

phase ($x = 0.33$, $T = 10$ K) there is no long bond: the refined local structure agrees with the average structure, there is no detectable structural disorder and no JT distortion [22]. There may be a suggestion of peak asymmetry on the Mn-O PDF peak at $r = 2.0$ Å (Fig. 1(b) and Fig. 2), and we cannot rule out the presence of large polarons [35]. However, there is no peak intensity around 2.15 Å , the position of the JT-long-bond in JT distorted material. As the MI transition is approached as a function of T and x , JT long-bonds appear, even in the FM phase. The long-bonds appear, not as a continuous elongation of the Mn-O long-bonds, but are apparent always at 2.15 Å and merely grow in intensity as the MI transition is approached. This is in qualitative agreement with our own neutron data and those of others [21], though Louca *et al.* present a different interpretation. It is also in agreement with XAFS data [13,14]. It is qualitatively, though not quantitatively, similar to the XAFS data of Lanzara *et al.* [35]. This is strong evidence for a microscopically inhomogeneous state in the ferromagnetic metallic region of the phase diagram, with a *microscopic* coexistence of localized JT and delocalized (Zener) material.

The PDF can *quantify* the relative proportion of the sample in each of these phases, even when there is no macroscopic phase separation. This is possible by monitoring the presence or absence of a Mn-O long-bond, or equivalently, by monitoring the width of the peak in the PDF originating from the O-O correlations in the MnO_6 octahedra. The PDF peak width is inversely proportional to its height and it is easier to monitor changes in peak-height. We can determine an excess peak height, h_{xs} , by subtracting an extrapolation to low temperature of the PDF peak-height from above T_c . This is shown in Fig. 4 for two data-sets. This preliminary result indicates that in $\text{La}_{1-x}\text{Ca}_x\text{MnO}_3$ the proportion of the sample in the delocalized phase may scale universally with reduced temperature close to T_c (Fig. 4, inset). From h_{xs} we obtain the proportion of the sample in the delocalized phase, $c(H, T)$, referred to as the “mixing factor” in Ref. [36]. Jaime *et al.* [36] make a prediction for the field and temperature dependence of $c(H, T)$, reproduced in Fig. 5, from their phenomenological model. This can be compared with the excess-PDF peak-height variation shown in Fig. 4(inset).

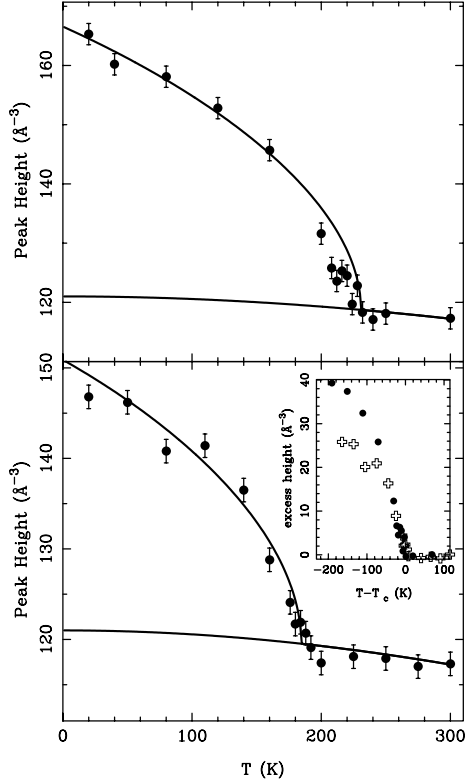


FIG. 4. O-O PDF Peak-height vs T from $\text{La}_{1-x}\text{Ca}_x\text{MnO}_3$. Top panel $x = 0.25$, bottom panel $x = 0.21$. Debye behavior has been fit to the high-temperature region. Excess-peak height is plotted vs. reduced temperature in the inset for $x = 0.25$ (circles) and $x = 0.21$ (crosses).

CONCLUSIONS

Using the PDF we can study the size and shape and presence and absence of the local Jahn-Teller distortions. We have carried out such an analysis on high real-space resolution x-ray diffraction data. We find that, deep in the ferromagnetic metallic phase there is no Jahn-Teller distortion and the sample is fully delocalized. As the MI transition is approached both with T and x , JT long-bonds appear indicating a microscopic coexistence of localized and delocalized material. The PDF can quantify the proportion of the sample in each phase. Preliminary results suggest that the quantity of delocalized sample seems to scale universally with reduced temperature.

ACKNOWLEDGEMENTS

This work was supported by NSF through grant DMR-9700966. CHESS is supported by NSF through grant DMR-9713424 and APS by DOE through grant W-31-109-Eng-38.

REFERENCES

1. A. P. Ramirez, J. Phys: Condens. Matter **9**, 8171 (1997).
2. C. Zener, Phys. Rev. **82**, 403 (1951).

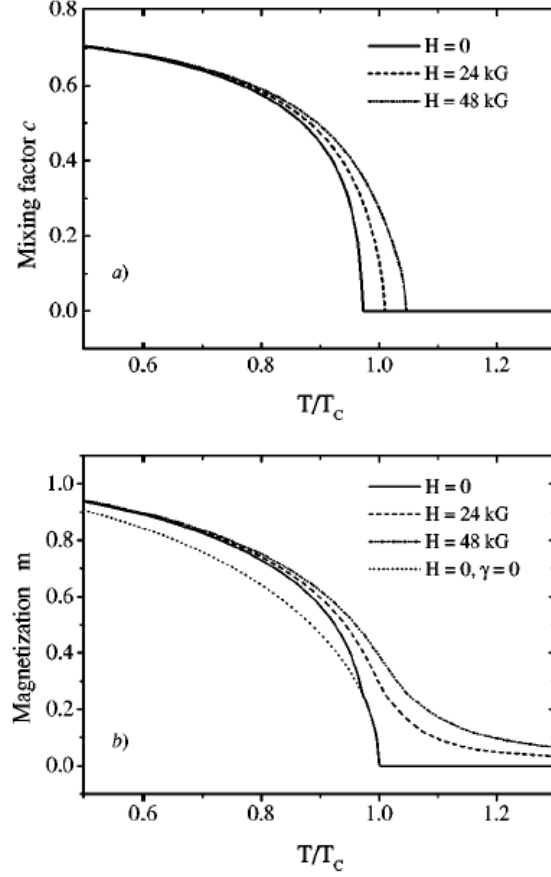


FIG. 5. Mixing factor $c(H, T)$ predicted for the proportion of the sample in the delocalized phase below T_c in the theory of Jaime *et al.* [36]

3. A. Chattopadhyay, A. J. Millis, and S. D. Sarma, Unpublished. (preprint: cond-mat/9908305).
4. A. J. Millis, P. B. Littlewood, and B. I. Shraiman, *Phys. Rev. Lett.* **74**, 5144 (1995).
5. A. J. Millis, *Nature* **392**, 147 (1998).
6. H. Röder, J. Zang, and A. R. Bishop, *Phys. Rev. Lett.* **76**, 1356 (1996).
7. A. Moreo, A. Yunoki, and E. Dagotto, *Science* **283**, 2034 (1999).
8. A. J. Millis, B. I. Shraiman, and R. Müller, *Phys. Rev. Lett.* **77**, 175 (1996).
9. J-S. Zhou, W. Archibald, and J. B. Goodenough, *Nature* **381**, 770 (1996).
10. A. S. Alexandrov and A. M. Bratkovsky, *Phys. Rev. Lett.* **82**, 141 (1999).
11. P. Dai, J. Zhang, H. A. Mook, S.-H. Liou, P. A. Dowben, and E. W. Plummer, *Phys. Rev. B* **54**, R3694 (1996).
12. S. J. L. Billinge, R. G. DiFrancesco, G. H. Kwei, J. J. Neumeier, and J. D. Thompson, *Phys. Rev. Lett.* **77**, 715 (1996).
13. C. H. Booth, F. Bridges, G. J. Snyder, and T. H. Geballe, *Phys. Rev. B* **54**, R15606 (1996).
14. C. H. Booth, F. Bridges, G. H. Kwei, J. M. Lawrence, A. L. Cornelius, and J. J. Neumeier, *Phys. Rev. B* **57**, 10440 (1998).
15. G. Zhao, K. Conder, H. Keller, and K. A. Müller, *Nature* **381**, 676 (1996).
16. G. M. Zhao, M. B. Hunt, and H. Keller, *Phys. Rev. Lett.* **78**, 955 (1997).
17. D. W. Visser, A. P. Ramirez, and M. A. Subramanian, *Phys. Rev. Lett.* **78**, 3947 (1997).
18. J. L. Cohn, J. J. Neumeier, C. P. Popoviciu, K. J. McCellan, and Th. Leventouri, *Phys. Rev. B* **56**, R8495 (1997).
19. M. Jaime, M. B. Salamon, M. Rubinstein, R. E. Treece, J. S. Horwitz, and D. B. Chrisey, *Phys. Rev. B* **54**, 11914 (1996).
20. M. Jaime, H. T. Hardner, M. B. Salamon, M. Rubinstein, P. Dorsey, and D. Emin, *Phys. Rev. Lett.* **78**, 951 (1997).
21. D. Louca, T. Egami, E. L. Brosha, H. Röder, and A. R. Bishop, *Phys. Rev. B* **56**, R8475 (1997).
22. S. J. L. Billinge, Th. Proffen, V. Petkov, J. Sarrao, and S. Kycia, submitted to *Phys. Rev. B*. (Preprint: cond-mat/9907329).
23. S. J. L. Billinge, in *Physics of Manganites*, page 201, Kluwer Academic/Plenum, 1999.
24. M. Uehara, S. Mori, C. H. Chen, and S.-W. Cheong, *Nature* **399**, 560 (1999).
25. D. E. Cox, P. G. Radaelli, M. Marezio, and S.-W. Cheong, *Phys. Rev. B* **57**, 3305 (1998).
26. Y. Waseda, *The structure of non-crystalline materials*, McGraw-Hill, New York, 1980.
27. V. Petkov, *J. Appl. Crystallogr.* **23**, 387 (1989).
28. Th. Proffen, R. G. DiFrancesco, S. J. L. Billinge, E. L. Brosha, and G. H. Kwei, *Phys. Rev. B* **60**, 9973 (1999).
29. S. J. L. Billinge, in *Local Structure from Diffraction*, edited by S. J. L. Billinge and M. F. Thorpe, page 137, New York, 1998, Plenum.
30. Th. Proffen and S. J. L. Billinge, *J. Appl. Crystallogr.* **32**, 572 (1999).
31. J. F. Mitchell, D. N. Argyriou, C. D. Potter, D. G. Hinks, J. D. Jorgensen, and S. D. Bader, *Phys. Rev. B* **54**, 6172 (1996).
32. Q. Huang, A. Santoro, J. W. Lynn, R. W. Erwin, J. A. Borchers, J. L. Peng, and R. L. Greene, *Phys. Rev. B* **55**, 14987 (1997).
33. J. Rodríguez-Carvajal, M. Hennion, F. Moussa, A. H. Moudden, L. Pinsard, and A. Revcolevschi, *Phys. Rev. B* **57**, R3189 (1998).
34. W. E. Pickett and D. J. Singh, *Phys. Rev. B* **53**, 1146 (1996).
35. A. Lanzara, N. L. Saini, M. Brunelli, F. Natali, A. Bianconi, P. G. Radaelli, and S. Cheong, *Phys. Rev. Lett.* **81**, 878 (1998).
36. M. Jaime, P. Lin, S. H. Chun, M. B. Salamon, P. Dorsey, and M. Rubinstein, *Phys. Rev. B* **60**, 1028 (1999).